

Semiempirical molecular orbital studies of the acylation step in the lipase-catalyzed ester hydrolysis

A. Jian-Hua Zhao,^a B. Hsuan-Liang Liu,^{a,b}

^a Department of Chemical Engineering and Biotechnology, National Taipei University of Technology, 1 Sec. 3 ZhongXiao E. Rd., Taipei, Taiwan 10608

^b Graduate Institute of Biotechnology, National Taipei University of Technology, 1 Sec. 3 ZhongXiao E. Rd., Taipei, Taiwan 10608

Abstract

In this study, we present the results from the semiempirical molecular orbital calculations for the acylation step in the lipase-catalyzed ester hydrolysis. The results reveal that the lowest energy path for the formation of the tetrahedral intermediate is for the serine residue of the catalytic triad to attack the substrate, followed by coupling heavy atom movement and proton transfer. The calculations of four active site models show that the cooperation of the aspartate group and the oxyanion hole is capable of lowering the activation energy by about 16 kcalmol⁻¹. Our results further suggest that the lipase-catalyzed ester hydrolysis adopts the single proton transfer mechanism.

Keywords: semiempirical molecular orbital calculations, acylation, lipase, oxyanion hole

1. Introduction

Lipases, a class of enzymes belonging to the serine hydrolases, have been proven to be efficient for resolving racemic alcohols and esters. Many lipases are heat-stable and can be used in organic solvents. It is of great interest to use molecular modeling for predicting the ability of these enzymes in discriminating the enantiomers of a particular substrate. So far, vast amounts of molecular modeling studies have been performed with the aim of rationalizing and/or predicting the enantioselectivity of triacylglycerol lipases toward various substrates.¹⁻⁵

It is well known that most lipases are functioned with the catalytic triad (Asp-His-Ser) located in the active site.⁶ The reason for this arrangement is presumably to make the Ser oxygen sufficiently nucleophilic before it attacks the carbonyl carbon of the amide or ester substrate. The most commonly accepted mechanism of serine hydrolases is divided into two steps: the acylation and the deacylation steps.⁷ The aim

of this study is to gain insights into the mechanistic aspect of the acylation step in the lipase-catalyzed ester hydrolysis using quantum chemical approaches. We further examined the effect of the Asp residue of the catalytic triad and the oxyanion hole on decreasing the activation energy by four active site models. Double proton transfer mechanism was also investigated in this study.

2. Methods

2.1 Preparation of the model protein

The crystal structure of the *Burkholderia Cepacia* lipase in complex with hexylphosphonic acid (R)-2-methyl-3-phenylpropyl ester (PDB code: 1YS1)⁶ was used to construct the lipase model. We further transformed (R)-2-methyl-3-phenylpropyl ester into methyl formate as the substrate used in our model by changing atom and bond types. This enzyme-substrate complex was then energy minimized using steepest decent method with 5000 steps, followed by conjugated gradient method with 5000 steps of the InsightII program (Silicon Graphics, Mountain View, CA).

2.2 Construction of the quantum mechanical active site model

After the structure of lipase was refined, the Cartesian coordinates of the catalytic triad (Ser87-His286-Asp264), the oxyanion hole (Leu17 and Gln88), and the substrate were extracted from the rest of the system for further quantum mechanical calculations. In our molecular orbital calculations, Ser87, His286, and Asp264 were modeled by methanol, imidazole, and formate anion, respectively. In addition, Leu17 and Gln88 were represented by two water molecules to mimic the formation of two hydrogen bonds with the carbonyl oxygen of the substrate.

2.3 Semiempirical calculations along reaction coordinate

Semiempirical molecular orbital calculations were carried out using the AM1⁸ and PM3⁹ molecular models, which are implemented within the MOPAC module in the InsightII program. All calculations of this study were made in gas phase. All the reactions were examined by using the reaction coordinate method¹⁰. The potential energy surface for the formation of the tetrahedral intermediate was calculated by restraining two reaction coordinates: 1) the distance between the hydroxyl oxygen of Ser and the carbonyl carbon of the substrate (R_a) and 2) the difference of the distances between the donating and the accepting oxygen atoms and the transferring proton (R_b), which describes the abstraction of a proton from the Ser oxygen to the His nitrogen. Full geometry optimization was accomplished by AM1 approach at each point along the reaction path, with the distance between the Ser hydroxyl oxygen and the carbonyl carbon of the substrate being fixed. Additionally, PM3 energies were also used to compute the AM1 optimized geometries (denoted as PM3//AM1). To investigate the double proton transfer mechanism, the reaction coordinate for a proton transfer from His to Asp was described by R_c , which is the difference of the distances between the donating and the accepting oxygen atoms and the transferring proton. Then, R_a and ($R_b + R_c$) were used to calculate the potential energy surface for the formation of TII in the double proton transfer mechanism.

3. Results and discussion

3.1 The acylation step and four active site models

The schematic representation for the acylation step of our model reaction is shown in Figure 1. The reaction begins from a near-attack complex in the acylation step (ES), which corresponds to the optimal Michaelis-Menten complex. The complex overcomes an energy barrier to reach the transition state (TS1), which involves a proton transfer from the Ser oxygen to the His nitrogen, resulting in a tetrahedral intermediate (TI1) and a protonated His group. To complete the acylation step, the His residue switches the hydrogen bond from the Ser oxygen to the methoxy oxygen of the ester to form TI2. The acyl-enzyme (EA) is subsequently formed due to a proton transfer from His to the methoxy group. Note that in our model, the potential energy surface is symmetric; i.e., ES and EA are considered to be the same species, so are TI1 and TI2, and TS1 and TS2. To further analyze the effect of the Asp group of the catalytic triad and the oxyanion hole on decreasing the activation energy, we dissected our FULL active site model (Figure 2A) into three partial models: 1) the ASP model in Figure 2B, 2) the 2W model in Figure 2C, and 3) the NO model in Figure 2D.

3.2 Semiempirical quantum mechanical calculations

The resulting three-dimensional potential energy surface after semiempirical quantum mechanical calculations is shown in Figure 3. It is of interest to note that the potential energy surfaces of the four models mentioned in Figure 2 exhibit similar lowest energy path for the formation of TI1. However, different activation energy barriers between ES and TS1 were observed for these models. For the FULL model (Figure 3A), the shape of the resulting potential energy surface shows two minima representing ES and TI1. The other two corners of the surface are the higher energy areas representing the unstable structures. The whole process can thus be illustrated as that the lowest energy path for the formation of TI1 is for Ser to attack the substrate, followed by coupling heavy atom movement and proton transfer. Some theoretical studies have indicated¹¹ or assumed¹² that the proton is transferred from Ser to His prior to attacking the substrate by Ser, such that the transferred proton is not a direct participant in the bond making and breaking events in the transition state. However, this sequence of steps is inconsistent with the experimental kinetic isotope effects suggesting that there is a protonic bridging in the transition state.¹³ In the FULL model, our results indicate that the Ser attack and proton transfer events occur simultaneously, indicating that there is a protonic bridging in the transition state, which is consistent with the previous experimental results.¹³

3.3 The effect of the Asp group of the catalytic triad and the oxyanion hole

The energies for the stationary points involved in the reaction are summarized in Table 1. It clearly indicates how the residues assist the enzymatic reaction by lowering the activation energy between ES and TS1. In the FULL model, the activation energy barriers are 21.1 and 30.6 kcalmol⁻¹ with AM1//AM1 and PM3//AM1, respectively. In the ASP model, the removal of two water molecules in the oxyanion hole raised the activation energy barriers by 3.6 and 8.8 kcalmol⁻¹ based

on AM1//AM1 and PM3//AM1, respectively, comparing to the FULL model. In the 2W model, the removal of Asp increased the activation energy barriers by 11.2 and 15.2 kcalmol⁻¹ with AM1//AM1 and PM3//AM1, respectively, comparing to the FULL model. Furthermore, in the NO model, the removal of both Asp and two water molecules in the oxyanion hole raised the activation energy barriers by 16 and 21.4 kcalmol⁻¹ with AM1//AM1 and PM3//AM1, respectively, comparing to the FULL model. Our results are in good agreement with previous theoretical study, suggesting that the exclusion of the electron correlation effects increases the activation energy barrier by 14 to 20 kcalmol⁻¹.¹⁴ It is noteworthy that the cooperation of Asp in the catalytic triad and the oxyanion hole is capable of stabilizing both TS1 and TI1, with the stabilizing effect more significant with TI1 than TS1. The results also indicate that a smaller activation energy barrier between ES and TS1 seems to yield a more stable TI1. Our results also suggest that the removal of Asp in the catalytic triad and the oxyanion hole drastically destabilizes TS1 and TI1 along the reaction pathway.

Some important geometrical parameters for the stationary points during the catalytic reaction are summarized in Table 2. The most representative bond lengths are probably d_4 , d_5 and d_6 . It is obvious that for all models studied here, the locations of TS1 and TI1 were almost the same. Additionally, the results also indicate that d_6 decreased significantly when the Ser oxygen approached the carbonyl carbon of the substrate, as the reaction reached TS1. A further slightly decrease in d_6 was observed when TI1 was formed, which was accompanied by proton transfer from Ser to His, with d_5 and d_4 being lengthened and shortened, respectively. At TI1, the proton has been transferred to His as can be seen from d_4 and d_5 . The hydrogen bonds between Asp and His (d_1 and d_2), and between two water molecules and ester (d_9 and d_{10}) also provide the description of the bonding natures of the stationary point studies. As the reaction proceeded, d_1 became shorter at TS1 and reached its shortest value at TI1. This can be attributed to proton transfer from Ser to His, which makes His more positively charged and further strengthens the bonding between Asp and His. The changes of d_9 and d_{10} along the reaction path are similar to that of d_1 , indicating that short hydrogen bonds were formed as the negative charges on the carbonyl oxygen were developed during the reaction. The length of the carbonyl bond (d_8) is another indication of the extent of the reaction. At ES, the bond length (about 1.23 Å) is of a typical carbonyl double bond. The C-O distance increased along the reaction path and reached its largest value in TI1, with d_8 being 1.29 Å. The geometrical arrangement at TI1 suggests that an anionic sp^3 tetrahedral intermediate is formed.

3.4 Double proton transfer mechanism

The double proton transfer mechanism of serine hydrolase catalysis proposed by Hunkapiller et al.¹⁵ involves the transfers of two protons in the transition state. In addition to proton transfer from Ser to His, the proton bonded on the other nitrogen of His is transferred to Asp. The tetrahedral intermediate in this mechanism thus consists of a neutral Asp group. Many quantum mechanical calculations employing a system composed entirely of the catalytic triad without the surrounding protein support the concerted double proton transfer mechanism.^{16,17} Although this mechanism is generally accepted for a number of years, experimental evidence since then has favored the single proton transfer mechanism.¹⁸⁻²¹ Recent NMR studies have suggested that the hydrogen bond between Asp and His is a low-barrier hydrogen

bond (LBHB),^{22,23} that can partially explain serine hydrolase catalysis. However, other NMR study²⁴ and theoretical calculations²⁵⁻²⁸ have argued against this hypothesis. The potential energy surface for the double proton transfer mechanism calculated in this study is shown in Figure 4. Our results show that the energy barrier is 33.6 kcalmol⁻¹ along the lowest energy path for the formation of TI1, which is significantly higher than that in the single proton transfer mechanism, indicating that the double proton transfer mechanism is disfavored for the lipase-catalyzed ester hydrolysis in terms of potential energy. In lipases, the Asp negative charge is generally stabilized by hydrogen bonds, e.g., in the *Burkholderia Cepacia*⁶ and the *Candida antartica* lipases²⁹, there are two and three hydrogen bonds formed with the Asp group, respectively. Thus, proton transfer from His to Asp seems to be unlikely due to the hydrogen bond stabilization.

4. Conclusions

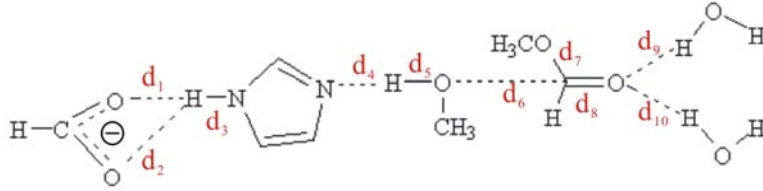
In this study, the semiempirical molecular orbital calculations were made to investigate the serine hydrolase catalyzed hydrolysis of ester and the effect of the Asp residue and oxyanion hole. These results show that the lowest energy pathway for formation of tetrahedral intermediate was Ser to approach the substrate, followed by coupled heavy atom movement and proton transfer to complete the reaction, which is consistent with previous experiments. Additionally, our result also suggests that the cooperation of the Asp group and oxyanion hole is capable of lowering the activation barrier by about 16 kcalmol⁻¹, indicating that the importance of Asp residue and oxyanion hole in catalytic mechanism of serine hydrolase. We also studied the double proton transfer mechanism. And the result shows the energy barrier in double proton transfer was higher than that in single proton transfer, indicating that the double proton transfer mechanism was disfavor in our calculations.

Table and figures

Table 1: Relative energies (kcalmol⁻¹) of TS1 and TI1 relative to ES calculated by AM1//AM1 and PM3//AM1.

	Model							
	FULL		ASP		2W		NO	
	TS1	TI1	TS1	TI1	TS1	TI1	TS1	TI1
AM1//AM1	21.05	9.09	24.66	15.62	32.22	30.99	37.07	36.71
PM3//AM1	30.56	13.53	39.40	25.89	45.71	38.47	51.96	47.23

Table 2. Geometrical parameters for the stationary points (ES, TS1, and TII) involved in the acylation step in different models.



Model	d ₁	d ₂	d ₃	d ₄	d ₅	d ₆	d ₇	d ₈	d ₉	d ₁₀
ES										
FULL	1.894	2.331	1.016	1.642	1.036	2.644	1.362	1.233	2.201	2.660
ASP	1.906	2.318	1.015	1.642	1.036	2.644	1.365	1.231	–	–
2W	–	–	0.985	1.642	1.036	2.644	1.358	1.234	2.209	2.196
NO	–	–	0.985	1.642	1.036	2.644	1.366	1.230	–	–
TS1										
FULL	1.838	2.351	1.025	1.342	1.336	1.544	1.414	1.278	2.099	2.084
ASP	1.848	2.349	1.023	1.342	1.336	1.544	1.424	1.269	–	–
2W	–	–	0.988	1.342	1.336	1.544	1.418	1.273	2.124	2.092
NO	–	–	0.988	1.242	1.436	1.544	1.434	1.265	–	–
TII										
FULL	1.762	2.348	1.037	1.042	1.636	1.444	1.443	1.290	2.077	2.067
ASP	1.797	2.341	1.034	1.042	1.636	1.444	1.457	1.280	–	–
2W	–	–	0.990	1.042	1.636	1.444	1.451	1.285	2.073	2.079
NO	–	–	0.990	1.042	1.636	1.544	1.444	1.266	–	–

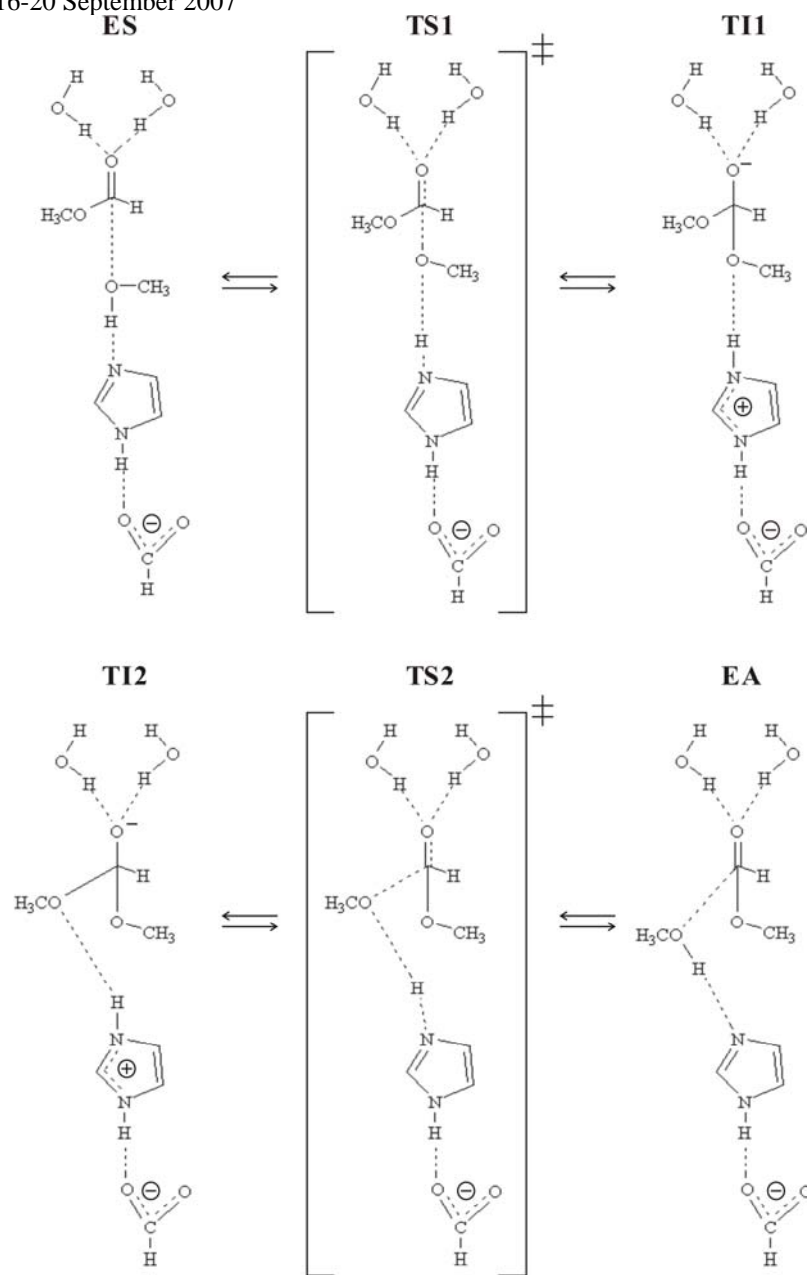


Figure 1: Schematic representation of the acylation step in the lipase-catalyzed ester hydrolysis.

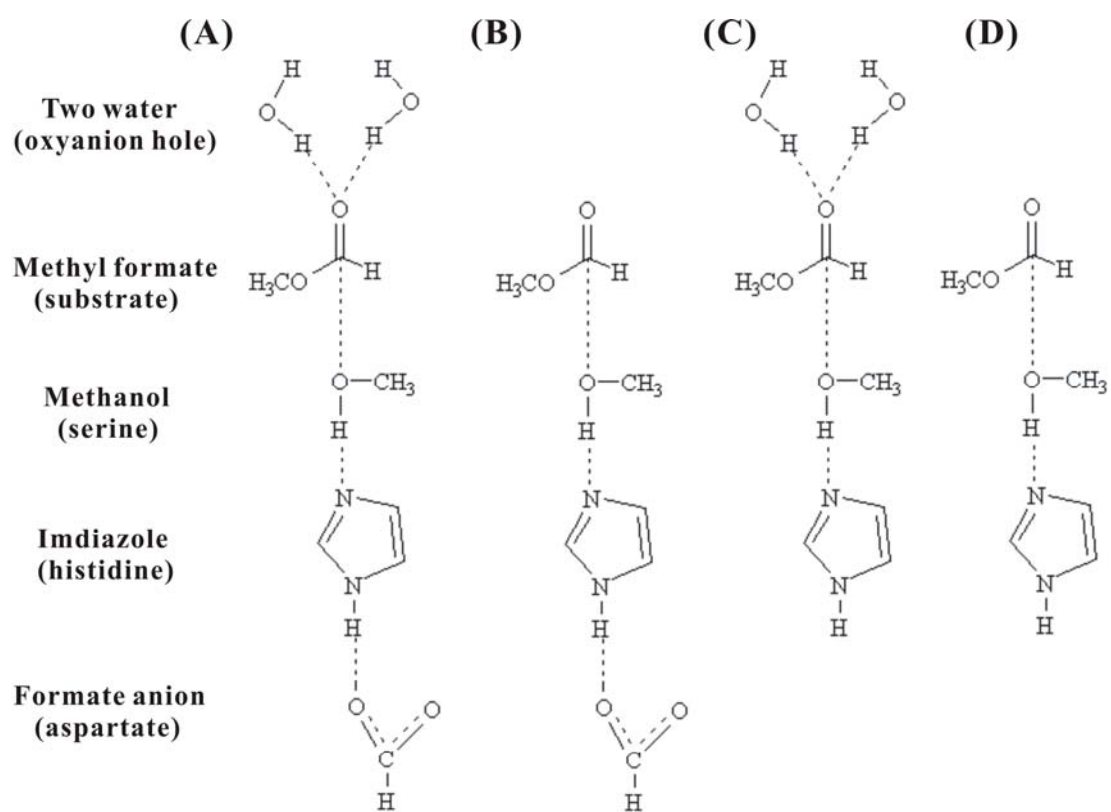
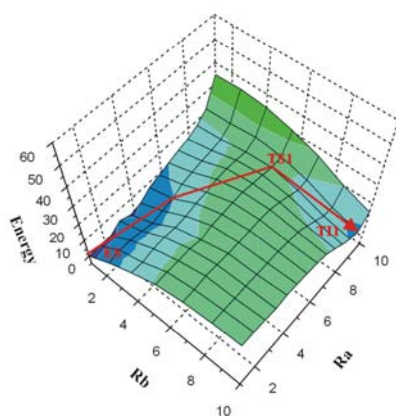
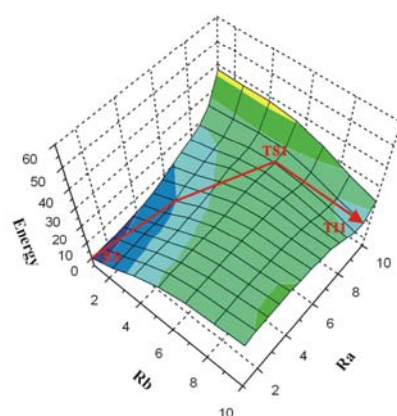


Figure 2: (A) FULL, (B) ASP, (C) 2W, and (D) NO model systems constructed in this study.

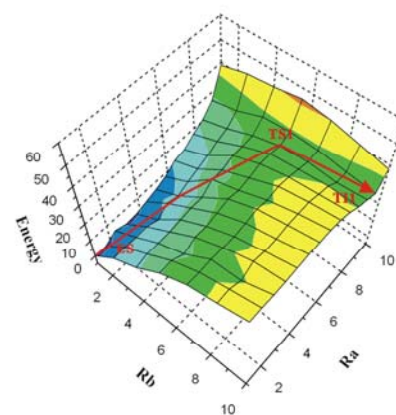
(A)



(B)



(C)



(D)

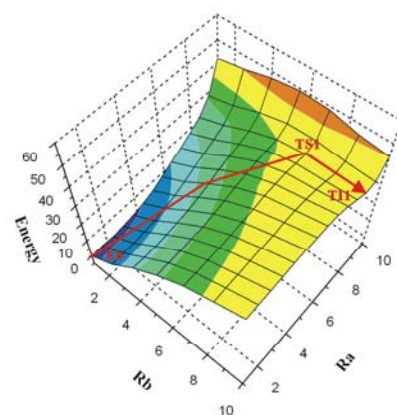


Figure 3: AM1//AM1 potential energy surfaces for the formation of TI1 in the acylation step described by the reaction coordinates R_a and R_b in the (A) FULL, (B) ASP, (C) 2W, and (D) NO models. Energies are given relative to ES in kcal mol^{-1} . For clarity, the reaction coordinates are labeled with the increment numbers rather than with the reaction coordinate values (e.g., '0' is the starting point of a particular coordinate). The energy bar is the same as in Figure 4. The lowest energy path is indicated by red arrow line for each plot, with the locations of ES, TS1, and TI1 labeled.

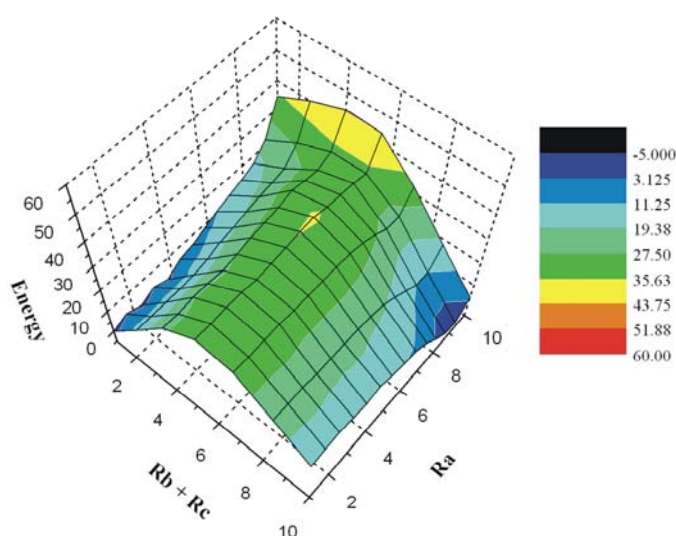


Figure 4: AM1//AM1 potential energy surface for the double proton transfer mechanism described by the reaction coordinates R_a and $(R_b + R_c)$ in the FULL model. Energies are given relative to ES in kcal mol^{-1} .

References

- (1) Holmquist, M., Häffner, F., Norin, T. and Hult, K., (1996) *Protein Sci.*, 5, 83-88.
- (2) Häffner, F., Norin, T., and Hult, K., (1998) *Biophys. J.*, 74, 1251-1262.
- (3) Tuomi, W. V. and Kazlauskas, R. J., (1999) *J. Org. Chem.*, 64, 2638-2647.
- (4) Scheib, H., Pleiss, J., Kovac, A., Paltauf, F. and Schmid, R. D., (1999) *Protein Sci.*, 8, 215-221.
- (5) Schulz, T., Pleiss, J. and Schmid, R. D., (2000) *Protein Sci.*, 9, 1053-1062.
- (6) Mezzetti, A. Schrag, J. D., Cheong, C.S. and Kazlauskas, R. J., (2005) *Chem. Biol.*, 12, 427-437.
- (7) Topf, M. and Richards, W. G., (2004) *J. Am. Chem. Soc.*, 126, 14631-14640.
- (8) Dewar, M. J. S., Zoebisch, E. G., Healy, E. F. and Stewart, J. J. P., (1985) *J. Am. Chem. Soc.*, 107, 3902-3909.
- (9) Stewart, J. J. P., (1989) *J. Comput. Chem.*, 10, 209-220.
- (10) Dewar, M. J. S. and Kirschner, S. J., (1971) *J. Am. Chem. Soc.*, 93, 4290-4291.
- (11) Scheiner, S. and Lipscomb, W., (1976) *Proc. Natl. Acad. Sci. USA*, 73, 432-436.
- (12) Warshel, A. and Russell, S., (1986) *J. Am. Chem. Soc.*, 108, 6569-6579.
- (13) Satterthwait, A. C. and Jencks, W. P., (1974) *J. Am. Chem. Soc.*, 96, 7018-7031.
- (14) Hu, C. -H., Brinck, T. and Hult, K., (1998) *Int. J. Quant. Chem.*, 69, 89-103.
- (15) Hunkapiller, M. W., Smallcombe, S. H., Whitaker, D. R. and Richards, J. H., (1973) *Biochemistry*, 12, 4732-4743.
- (16) Umeyama, H., Imamura, A., Nagato, C. and Hanano, M., (1973) *J. Theor. Biol.*, 41, 485-502.
- (17) Scheiner, S., Kleier, D. A. and Lipscomb, W. N., (1975) *Proc. Natl. Acad. Sci. USA*, 72, 2606.

Semiempirical molecular orbital studies of the acylation step in the lipase-catalyzed ester hydrolysis
Proceedings of European Congress of Chemical Engineering (ECCE-6)
Copenhagen, 16-20 September 2007

- (18) Bachovchin, W. W. and Roberts, J. D., (1978) *J. Am. Chem. Soc.*, 100, 8041-8047.
- (19) Bachovchin, W. W., Kaiser, R., Richards, J. H. and Roberts, J. D., (1981) *Proc. Natl. Acad. Sci. USA*, 78, 7323-7326.
- (20) Kossiakoff, A. A. and Spencer, S. A., (1981) *Biochemistry*, 20, 6462-6474.
- (21) Bachovchin, W. W., (1986) *Biochemistry*, 25, 7751-7759.
- (22) Cleland, W. W. and Kreevoy, M. M., (1994) *Science*, 264, 1887-1890.
- (23) Frey, P. A., Whitt, S. A. and Tobin, J. B., (1994) *Science*, 264, 1927-1930.
- (24) Ash, E.L., Sudmeier, J. L., De Fabo, E. C. and Bachovchin, W. W., (1997) *Science*, 278, 1128-1132.
- (25) Warshel, A. and Papazyan, A., (1996) *Proc. Natl. Acad. Sci. USA*, 93, 13665-13670.
- (26) Topf, M., Varnai, P. and Richards, W.G., (2002) *J. Am. Chem. Soc.*, 124, 14780-14788.
- (27) Westler, W. M. Weinhold, F. and Markley, J. L., (2002) *J. Am. Chem. Soc.*, 124, 14373-14381.
- (28) Schutz, C.N. and Warshel, A., (2004) *Proteins: Struct. Funct. Bioinformatics*, 55, 711-723.
- (29) Uppenberg, J., Hansen, M. T., Patkar, S. and Jones, T. A. (1994) *Structure*, 2, 293-308.